Sensitivity and Linearity of Superconducting Radio-Frequency Single-Electron Transistors: Effects of Quantum Charge Fluctuations

Madhu Thalakulam,[1,2] Z. Ji,[1] and A. J. Rimberg[1,2,3]

[1]*Department of Physics and Astronomy, Rice University, Houston, Texas 77005, USA*
[2]*Rice Quantum Institute, Rice University, Houston, Texas 77005, USA*
[3]*Department of Electrical and Computer Engineering, Rice University, Houston, Texas 77005, USA*
(Received 14 October 2003; published 5 August 2004)

We have investigated the effects of quantum fluctuations of quasiparticles on the operation of superconducting radio-frequency single-electron transistors (rf-SETs) for large values of the quasiparticle cotunneling parameter $\alpha = 8E_J/E_c$, where E_J and E_c are the Josephson and charging energies. We find that, for $\alpha > 1$, subgap rf-SET operation is still feasible despite quantum fluctuations that wash out quasiparticle tunneling thresholds. Surprisingly, such rf-SETs show linearity and signal-to-noise ratio superior to those obtained when quantum fluctuations are weak, while still demonstrating excellent charge sensitivity.

The radio-frequency single electron transistor (rf-SET) is a highly sensitive, fast electrometer, and has been suggested as a potentially quantum-limited linear amplifier suitable for measurements of individual electronic charges [1–4]. Recent investigations have addressed use of the rf-SET as an electrometer [4–6], a readout device for charge based qubits [7–9], and a sensor for real-time electron counting experiments [10]. Linearity is a fundamental assumption of theoretical discussions of the quantum limits of amplifiers [1,11]. Nonetheless, there has been no detailed investigation of the range of linear response for the rf-SET.

Most theoretical studies of rf-SET performance focus on normal metal SETs, either in the sequential tunneling [1,12,13] or cotunneling regimes [2], while most experiments are performed using a superconducting SET (SSET) [6–8,10]. Transport in the SSET can be divided into two regimes, depending on the relative sizes of the bias voltage V_{dc} and superconducting gap Δ: above gap ($eV_{dc} > 4\Delta$), dominated by Coulomb blockade of quasiparticles, and subgap ($eV_{dc} < 4\Delta$), dominated by combinations of quasiparticle (QP) and resonant Cooper pair tunneling known as Josephson-quasiparticle (JQP) cycles [14,15]. While the best charge sensitivities are found for above-gap operation [6], the SSET backaction—the rate at which it dephases a measured system—is largest there [1,3,9]. Recent work has focused on subgap operation for which backaction is significantly reduced, and shot noise is non-Poissonian [3,7,16]. Theoretical studies of quantum fluctuations in the SSET have been limited to above-gap cotunneling of quasiparticles [17]. In this Letter we find that linearity and subgap quantum charge fluctuations in superconducting rf-SETs are intimately related: as quantum fluctuations strengthen, linearity and signal-to-noise ratio (SNR) improve, while charge sensitivity remains excellent.

Our SSETs consist of a small island connected to macroscopic leads via two Al/AlO$_x$/Al tunnel junctions J1(2) with normal state resistances $R_{1(2)}$ as illustrated in Fig. 1(a). We have fabricated and characterized three samples, S1, S2, and S3 with total resistance $R_n = R_1 + R_2$ of 58, 38, and 24 kΩ; an electron micrograph of S2 is shown in Fig. 1(b). Results similar to those described here were previously observed in four other samples [18]. The samples were mounted on the mixing chamber of a dilution refrigerator at its base temperature of 20 mK. High-frequency noise was excluded by π-type filters at
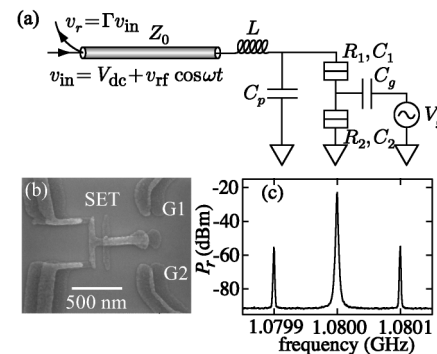

FIG. 1. (a) Schematic diagram of rf-SET operation. A voltage v_{in} consisting of dc and rf biases V_{dc} and v_{rf} is incident on a tank circuit comprising an inductor L, a capacitor C_p, and the SET, with junction resistances and capacitances $R_{1(2)}$ and $C_{1(2)}$. A charge oscillation $q_0 \cos\omega_m t$ modulates the reflection coefficient Γ of the tank circuit and the reflected voltage v_r. (b) Post-measurement electron micrograph of S2. Gates G1 and G2 were used vary the SET offset charge. (c) Power spectrum of v_r for $q_0 = 0.063e$ rms and $\omega_m/2\pi = 100$ kHz. The charge sensitivity and SNR of the rf-SET were determined from the sideband power and noise floor; the latter, dominated by the white noise of a cryogenic amplifier, was independent of sample, bias, and offset charge.

room temperature, and both copper powder and lossy transmission line filters in the cryostat. Total attenuation for frequencies above 1 GHz was $\gtrsim 170$ dB, of which $\gtrsim 120$ dB was at the mixing chamber temperature. A Nb chip inductor $L \approx 120$ nH together with the parasitic capacitance $C_p \approx 0.2$ pF of the SET contacts constituted a tank circuit with resonant frequency $f_{LC} \approx 1$ GHz and quality factor $Q \approx 16$. We measured the samples' current-voltage (I-V) characteristics in an asymmetric voltage-biased configuration [Fig. 1(a)] by varying the dc bias voltage V_{dc} in the absence of an rf excitation. Details of rf operation are discussed elsewhere [4,6]. The SET offset charge $Q_0 + q_0 \cos \omega_m t$ consisted of a dc component Q_0 that set the overall working point and an ac component of amplitude q_0 that modulated the reflected voltage v_r. Power spectra of v_r [Fig. 1(c)] were used to determine the charge sensitivity δq and SNR.

In Fig. 2, we show I-V characteristics of the samples for different Q_0, with $q_0 = 0$. For S1, we observe clear above gap ($V_{dc} \gtrsim 800$ μV) current modulation corresponding to Coulomb blockade of QP tunneling [Fig. 2(a)]. The sub-gap features corresponding to the JQP [14,15] cycles are sharp and clearly distinguished. As illustrated in Fig. 3, the simplest JQP cycle consists of resonant tunneling of a Cooper pair through one junction and two QPs through the other, transporting two electrons through the SET. The cycle can occur only when the transition $0 \rightarrow 1$ ($1 \rightarrow 0$) is allowed, i.e., for $eV_{dc} > E_c + 2\Delta$ where $E_c = e^2/2C_\Sigma$ is the charging energy of the SET and $C_\Sigma = C_1 + C_2 + 2C_g$ its total capacitance. While the JQP cycle is forbidden at lower bias, at $Q_0/e = n_g \approx \frac{1}{2}$ and $eV_{dc} =$

$2E_c$ Cooper pair tunneling is resonant at both junctions and the double JQP (DJQP) cycle becomes possible. The fact that sequential tunneling cannot occur via either cycle for $2E_c \lesssim eV_{dc} \lesssim E_c + 2\Delta$ is reflected in S1 by a sharp drop in current at $V_{dc} \approx 630$ μV just below the JQP feature.

As R_n decreases, so does current modulation for $eV_{dc} > 4\Delta$, consistent with suppression of the Coulomb blockade by QP cotunneling [17]: the modulation is reduced for S2, and nearly absent for S3 [Figs. 2(b) and 2(c)]. In contrast, features corresponding to the JQP cycles still exist but become progressively less sharp. Since these cycles involve both Cooper pair and QP tunneling, we hypothesize that subgap quantum fluctuations of quasiparticles are strong, while quantum fluctuations of Cooper pairs remain weak. Since to the best of our knowledge no theoretical description of subgap quantum charge fluctuations in the SSET exists, we provide simple arguments supporting our hypothesis.

We first compare with known results for above-gap transport. We define [17] a parameter $\alpha \equiv \frac{\Delta}{E_c}(\pi\hbar/e^2) \times (R_1^{-1} + R_2^{-1}) = (8E_J/E_c)$ characterizing the strength of quantum fluctuations for QPs, assuming $R_{1(2)} = R_n/2$ and using the Ambegaokar-Baratoff relation for the Josephson coupling energy $E_J = \frac{\Delta}{4}(R_K/R_n)$ where $R_K = \frac{h}{e^2}$. Quantum fluctuations are negligible for $\alpha \ll 1$. Determining E_c from the location of the DJQP peak and E_J from the total junction resistance we calculate α as in Table I. None of our samples satisfies $\alpha \ll 1$, although for S1 ($\alpha = 0.78$) some above-gap Coulomb
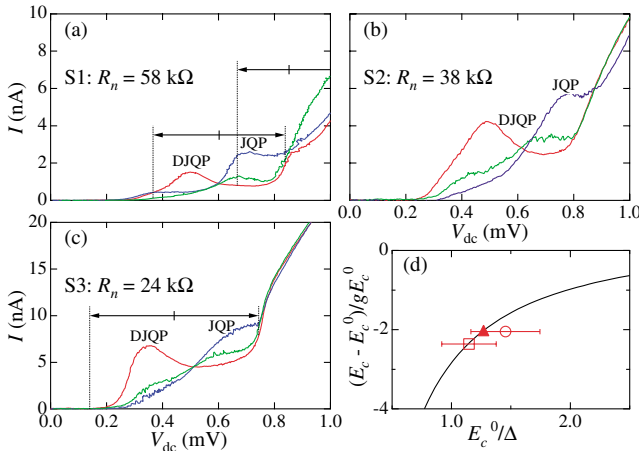

FIG. 2 (color online). *I*-*V* characteristics for (a) S1 (b) S2 and (c) S3 (note scale change), were chosen for Q_0 showing the DJQP process (red or gray), the JQP process (blue or dark gray), and an intermediate value of Q_0 (green or light gray). The arrows and vertical hash marks show the peak-to-peak rf amplitude $2Qv_{rf}$ and dc bias V_{dc} for optimal rf-SET operation. (d) Variation in the measured charging energy E_c relative to the bare charging energy E_c^0 for S1 (solid triangle), S2 (circle), and S3 (square). Error bars indicate uncertainty in E_c^0. Solid line: theoretical prediction.
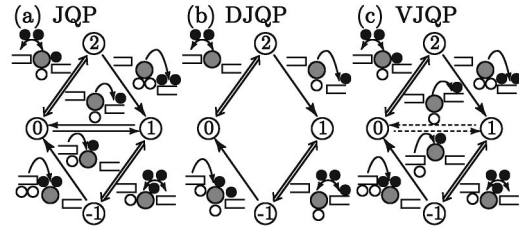

FIG. 3. Various JQP cycles. Here J2(1) is on the left (right) and $V_{dc} > 0$. Solid (empty) circles indicate quasielectrons (quasiholes) created during a cycle. The gray circles (white rectangles) indicate the SET island (leads) and their vertical separation the free energy difference for the transition. Cooper pair, quasiparticle, and virtual tunneling are indicated by double, single, and dashed arrows. (a) JQP cycle. Beginning in the state $n = 0$ ($n = 1$), where n is the number of excess electrons on the SET, the transition $0 \rightarrow 1$ ($1 \rightarrow 0$) is allowed, bringing Josephson tunneling through J1(2) into resonance. Cooper pair tunneling $1 \Leftrightarrow -1$ ($0 \Leftrightarrow 2$) is interrupted by QP tunneling through the opposite junction $-1 \rightarrow 0$ ($2 \rightarrow 1$), completing the cycle. (b) DJQP cycle. When Josephson tunneling is resonant for both J1 and J2, transport occurs via the sequence $0 \Leftrightarrow 2$, $2 \rightarrow 1$, $1 \Leftrightarrow -1$, $-1 \rightarrow 0$. (c) Proposed VJQP cycle. If the transition $0 \rightarrow 1$ ($1 \rightarrow 0$) is forbidden, it may still occur virtually. The remaining JQP transitions are allowed for relevant V_{dc}.

modulation survives. The progressively weakening modulation for S2 ($\alpha = 1.08$) and S3 ($\alpha = 2.65$), is consistent with previous results [17].

Cotunneling as described in Ref. [17] occurs only for $V_{dc} > 4\Delta/e$: it results in two QP excitations and transfers a single electron through the SET. Other virtual processes, however, remain important for $V_{dc} < 4\Delta/e$. For normal SETs, E_c is renormalized by quantum charge fluctuations: e.g., near $n_g = 0$, the effective charging energy $E_c \approx E_c^0(1 - 4g)$ where $g = R_K/\pi^2 R_n$ is the dimensionless parallel conductance of the tunnel junctions and E_c^0 the bare charging energy; similar renormalization occurs in SSETs [5,19]. Calculating the first-order energy shift due to transitions $n \to n \pm 1$, we find the renormalized charging energy $E_c^s = E_c^0[1 + g(\Delta/E_c^0) \times \{\Gamma[(E_c^0/\Delta)(1 + 2n_g)] + \Gamma[(E_c^0/\Delta)(1 - 2n_g)]\}]$ where $\Gamma(x) = \int_0^\infty K_1^2(u)e^{-xu}\,du$ and $K_1(u)$ is a Bessel function.

Using the expression for E_c^s, we find empirically that $E_c^0 = 254\ \mu eV$ gives the measured E_c for S1. We measure the total geometric junction area A_{tot} for the samples with an estimated accuracy of $\pm 20\%$, obtaining the values in Table I. Setting $E_c^0 = e^2/2C_\Sigma^0$ where $C_\Sigma^0 = C_1^0 + C_2^0 + 2C_g$ and using $2C_g \approx 80$ aF, we obtain $C_1^0 + C_2^0 = 195$ aF as the total unrenormalized junction capacitance for S1. Scaling this result according to A_{tot} we find C_Σ^0, E_c^0 and finally E_c^s for S2 and S3 [Table I]; agreement is excellent given the uncertainties in A_{tot}. Because of slightly heavier oxidation, S1 has both larger R_n and A_{tot} than S2. Since R_n varies exponentially with oxide thickness and $C_1^0 + C_2^0$ only linearly, the simple scaling with A_{tot} used here seems reasonable. Figure 2(d) shows the relative difference between E_c and E_c^0 scaled by $1/g$. The results agree with theory to within our experimental accuracy, and are consistent with the presence of subgap quantum fluctuations of QPs in our samples.

Virtual QP tunneling may also play a role in subgap transport, as suggested by the softening of the JQP cycle cutoff in S2 and S3. To illustrate such effects more clearly we show a plot of the $I(V_{dc}, n_g)$ surface for S2 in Fig. 4(a). The JQP resonances along the $0 \Leftrightarrow 2$ and $1 \Leftrightarrow -1$ lines and the DJQP peak at their intersection are clearly visible, but there is no sharp cutoff of the JQP process below the $1 \to 0$ $(0 \to 1)$ thresholds. To rule out extrinsic effects such as self-heating or high-frequency noise, we show in Fig. 4(b) a simulation of the current in S2 based on sequential tunneling [20] at an elevated temperature and including photon-assisted tunneling due to an electromagnetic environment with effective temperature $T_{env} =$

1 K. Despite the extreme conditions the QP tunneling thresholds are clearly visible in the simulation, and the SSET current drops nearly to zero between the JQP and DJQP features. The absence of QP thresholds in Fig. 4(a) is intrinsic to the sample and calls for an explanation outside of the sequential tunneling picture.

We therefore propose a process that could allow transport along the Cooper pair resonance lines between the JQP and DJQP features as illustrated schematically in Fig. 3(c). If below threshold the transition $1 \to 0$ $(0 \to 1)$ occurs virtually, the transitions $0 \Leftrightarrow 2$ and $2 \to 1$ $(-1 \Leftrightarrow 1$ and $1 \to 0)$ are allowed, completing what we call the virtual JQP (VJQP) cycle. Similar "shake-up" processes have been discussed for normal-metal tunnel junction systems [21]. Two QP excitations are created, but two electrons are transferred through the SET, so that the VJQP process is allowed for $eV > 2\Delta$. The energy barrier E_b for $1 \to 0$ $(0 \to 1)$ vanishes at threshold and climbs to $E_b \approx E_c + 2\Delta$ at the DJQP peak. The process can be neglected if the allowed QP tunneling rate Γ_{qp} is small compared to the inverse dwell time of the virtual quasiparticle: $\Gamma_{qp} \ll E_b/\hbar$. Using $\Gamma_{qp} = 4\Delta/e^2 R_n$, this becomes $R_n \gg (R_K/\pi)(2\Delta/E_b)$, which is violated for a range of voltages between the DJQP and JQP features. A detailed theoretical analysis is required to determine the contribution of the VJQP cycle to transport.

In contrast to the QP thresholds, features associated with Cooper pair tunneling are visible in both the data and the simulation, suggesting that the number of Cooper pairs is well defined. For the JQP process at resonance, the Cooper pair tunneling rate is $\Gamma_{cp} \approx E_J^2/\hbar\Gamma_{qp} = \frac{\pi}{8}(E_J/\hbar)$ [22]. Demanding that energy broadening due to Cooper pair tunneling be small compared to the typical energy barrier $4E_c$ for virtual tunneling gives $2\hbar\Gamma_{cp}/4E_c = (\pi/16)(E_J/E_c) \ll 1$, which is easily satisfied even for S3. For S2 and S3, then, quantum fluctuations are significant for QPs but small for Cooper pairs.

We now turn to rf operation. Optimal operating conditions were selected as follows: a small charge oscillation $q_0 \approx 0.006e$ rms was applied and the SNR determined from the power spectrum of ν_r as in Fig. 1(c). Subgap operation (all samples) and above-gap
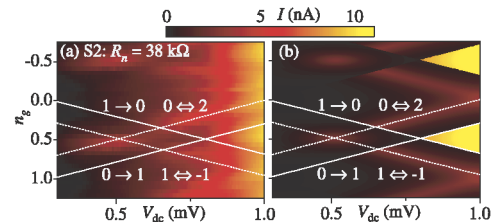

FIG. 4 (color online). False color or gray scale images of $I(V_{dc}, n_g)$ for (a) S2 at $T = 20$ mK, and (b) a simulation at $T = 200$ mK assuming an electromagnetic environment with impedance $R_{env} = 50\ \Omega$ and temperature $T_{env} = 1$ K. Cooper pair resonance lines $0 \Leftrightarrow 2$ ($-1 \Leftrightarrow 1$) and QP tunneling thresholds $1 \to 0$ $(0 \to 1)$ are indicated by the dashed and solid lines.

TABLE I. Sample parameters. Resistances are in $k\Omega$, energies in μeV, and areas in $10^{-3}\ \mu m^2$.

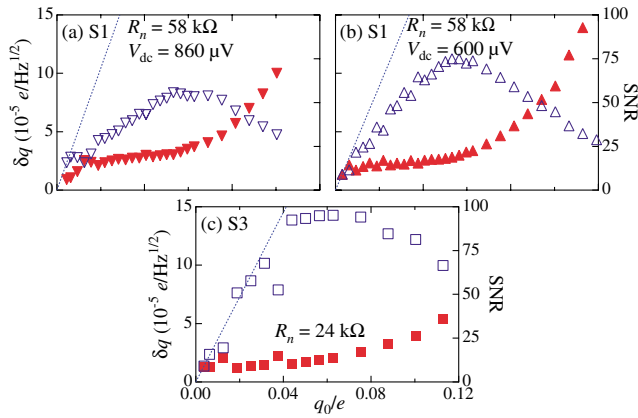|	R_n	Δ	E_c	E_J	α	A_{tot}	E_c^0	E_c^s
S1	58	200	230	22	0.78	4.1	254	
S2	38	200	250	34	1.08	3.4	291	258
S3	24	190	162	54	2.65	5.0	218	162

FIG. 5 (color online). Charge sensitivity δq and SNR (linear scale) versus q_0 in e rms for (a) S1, above-gap, (b) S1, subgap, and (c) S3, subgap. Charge sensitivity (solid red symbols) is plotted on the left axis and SNR (open blue symbols) on the right. For reference, the SNR for linear response is plotted as the dashed lines for δq measured at the smallest q_0.

operation (S1) were optimized over dc bias V_{dc}, rf bias v_{rf} and offset charge Q_0. We measured SNR versus input amplitude q_0 for each optimization and determined the charge sensitivity δq using $\delta q = (q_0/\sqrt{BW})10^{-SNR/20}$ where the resolution bandwidth BW $= 1$ kHz and SNR is in dB [6].

The optimized biases for S1 and S3 are indicated in Fig. 2 and the results of the δq and SNR measurements in Fig. 5. For S1 the best $\delta q = 9 \times 10^{-6}$ $e/\sqrt{Hz}$ was found for $V_{dc} = 860$ µV, consistent with previous results [6]. Linearity, however, was poor: as q_0 increases, the measured SNR rapidly becomes sublinear, and δq worsens [Fig. 5(a)]. Since δq does not saturate even for $q_0 = 4.5 \times 10^{-3}e$ rms it is unclear how small q_0 must be to achieve linear response. For subgap operation ($V_{dc} = 600$ µV) of S1 [Fig. 5(b)], we find $\delta q \approx 1.3 \times 10^{-5}$ $e/\sqrt{Hz}$, with SNR nearly linear to $q_0 \lesssim 0.01e$ rms. Since δq appears close to saturation at $q_0 = 3.1 \times 10^{-3}e$ rms, we may have approached linear response.

For S3 the best operating point occurred at $V_{dc} = 440$ µV [Fig. 5(c)], between the DJQP and JPQ features with $\delta q \approx 1.2 \times 10^{-5}$ $e/\sqrt{Hz}$, better than that for subgap operation of S1. Moreover, linearity was vastly improved: the SNR remains linear and δq nearly flat to $q_0 = 0.038e$ rms indicating that we have achieved linear response in this sample. For S2 (data not shown) the best $\delta q \approx 1.2 \times 10^{-5}$ $e/\sqrt{Hz}$ also occurred subgap, and the SNR was linear to $q_0 \approx 0.02e$ rms.

We can now make some general statements about the effects of quantum fluctuations on rf-SET operation. For samples with smaller α such as S1, transport is fairly well described by the sequential tunneling picture: I-V characteristics are sharp and vary strongly with Q_0 giving rise to excellent charge sensitivity. The same sharpness, however, prevents good linearity, since a large q_0 necessarily moves the SET far from optimal operation. For samples with larger α such as S3, quantum fluctuations causes at

least two important effects. First, the subgap features are smoothed and broadened, improving linearity: e.g., in S3 there is no "dead spot" between the DJQP and JQP features for which the SSET current is roughly independent of Q_0. Second, the smaller R_n simplifies impedance matching between the rf-SET and the 50 Ω coaxial line.

In conclusion, we have investigated the influence of quantum charge fluctuations on the charge sensitivity and SNR of rf-SETs. We find that rf-SETs with $\alpha \gtrsim 1$–2 (strong quantum fluctuations) show both good linearity and good charge sensitivity. In contrast, rf-SETs with $\alpha < 1$ (weak quantum fluctuations) show poor linearity and only modestly better charge sensitivity. These findings assume particular importance given interest in the rf-SET as a potentially quantum-limited linear amplifier. We have achieved linear response only for subgap operation in samples with $\alpha \gtrsim 1$ for which quantum fluctuations of quasiparticles are substantial.

[1] M. H. Devoret and R. J. Schoelkopf, Nature (London) **406**, 1039 (2000).
[2] A. Maassen van den Brink, Europhys. Lett. **58**, 562 (2002).
[3] A. A. Clerk et al., Phys. Rev. Lett. **89**, 176804 (2002).
[4] R. J. Schoelkopf et al., Science **280**, 1238 (1998).
[5] K. W. Lehnert et al., Phys. Rev. Lett. **91**, 106801 (2003).
[6] A. Aassimee et al., Appl. Phys. Lett. **79**, 4031 (2001).
[7] K. W. Lehnert et al., Phys. Rev. Lett. **90**, 027002 (2003).
[8] A. Aassime et al., Phys. Rev. Lett. **86**, 3376 (2001).
[9] Yu. Makhlin, G. Schön, and A. Shnirman, Rev. Mod. Phys. **73**, 357 (2001).
[10] W. Lu et al., Nature (London) **423**, 422 (2003).
[11] C. M. Caves, Phys. Rev. D **26**, 1817 (1982).
[12] A. N. Korotkov and M. A. Paalanen, Appl. Phys. Lett. **74**, 4052 (1999).
[13] G. Johansson, A. Käck, and G. Wendin, Phys. Rev. Lett. **88**, 046802 (2002).
[14] T. A. Fulton et al., Phys. Rev. Lett. **63**, 1307 (1989).
[15] A. Maassen van den Brink, G. Schön, and L. J. Geerligs, Phys. Rev. Lett. **67**, 3030 (1991).
[16] M. S. Choi, F. Plastina, and R. Fazio, Phys. Rev. Lett. **87**, 116601 (2001).
[17] D. V. Averin et al., Phys. Rev. Lett. **78**, 4821 (1997).
[18] W. Lu, Ph.D. thesis, Rice University, Houston, TX, 2003.
[19] P. Joyez et al., Phys. Rev. Lett. **79**, 1349 (1997).
[20] W. Lu, K. D. Maranowski, and A. J. Rimberg, Phys. Rev. B **65**, 060501 (2002).
[21] D. V. Averin, A. A. Odintsov, and S. V. Vyshenskii, J. Appl. Phys. **73**, 1297 (1993).
[22] D. V. Averin and V. Ya. Aleshkin, Pis'ma Zh. Eksp. Teor. Fiz. **50**, 331 (1989) [JETP Lett. **50**, 367 (1989)].